

Synthesis of bimetallic nickel cobalt selenide particles for high-performance hybrid supercapacitors

Bei Jiang,^{a,b} Yang Liu,^{a,b} Jingchao Zhang,^b Yinhuan Wang,^b Xinyu Zhang,^b Renchun Zhang,^b Liang-Liang Huang,^{a*} Daojun Zhang^{b*}

^a School of Chemistry and Material Science, Liaoning Shihua University, Fushun 113001, Liaoning, P. R. China. E-mail: huangll@lnpu.edu.cn

^b College of Chemistry and Chemical Engineering, Anyang Normal University, Anyang 455000, Henan, China. E-mail: zhangdj0410@sohu.com

2.6 Physical Characterization Techniques

The morphology of the series of nickel cobalt selenide particles are characterized by field-emission scanning electron microscopy (FESEM, HITACHI, SU8010) and transmission electron microscopy (TEM, FEI TECNAI G2 TF20). X-ray diffraction (XRD) of these samples were obtained on a PANalytical X-ray diffractometer. X-ray photoelectron spectroscopy (XPS, Thermo 250Xi) is used to study the chemical valence states of the best performed $\text{Ni}_{0.95}\text{Co}_{2.05}\text{Se}_4$ sample.

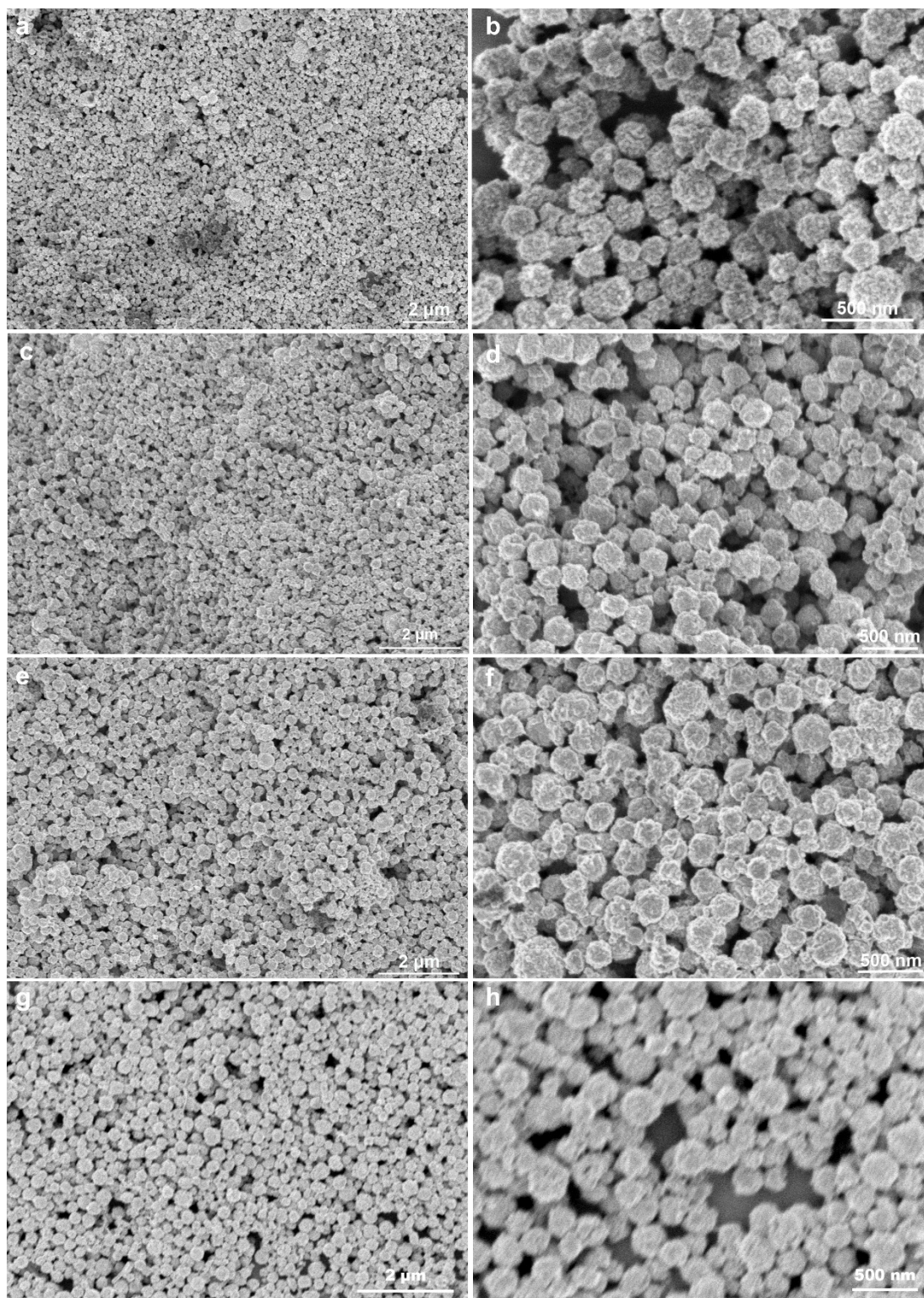


Fig. S1. SEM images of different samples. (a-b) Co_3Se_4 , (c-d) $\text{Ni}_{1.14}\text{Co}_{1.86}\text{Se}_4$, (e-f) $\text{Ni}_{0.67}\text{Co}_{2.33}\text{Se}_4$, (g-h) $\text{Ni}_{0.53}\text{Co}_{2.47}\text{Se}_4$.

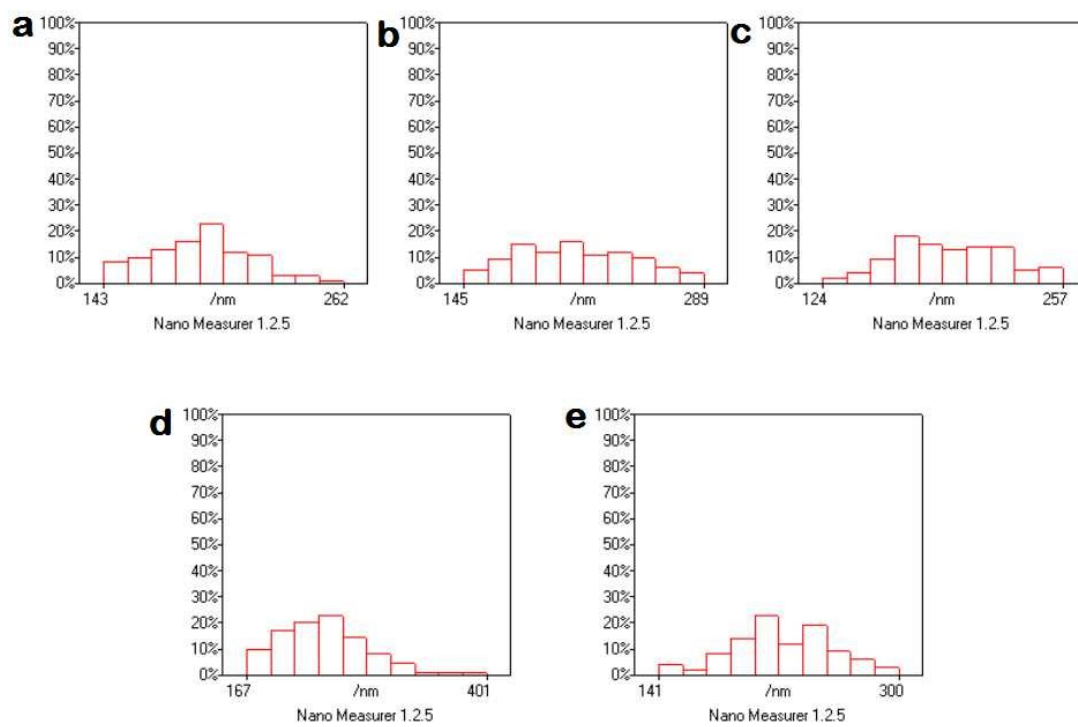


Fig. S2. A column chart of the size distribution of different samples. (a) Co_3Se_4 , (b) $\text{Ni}_{1.14}\text{Co}_{1.86}\text{Se}_4$, (c) $\text{Ni}_{0.95}\text{Co}_{2.05}\text{Se}_4$, (d) $\text{Ni}_{0.67}\text{Co}_{2.33}\text{Se}_4$, (e) $\text{Ni}_{0.53}\text{Co}_{2.47}\text{Se}_4$.

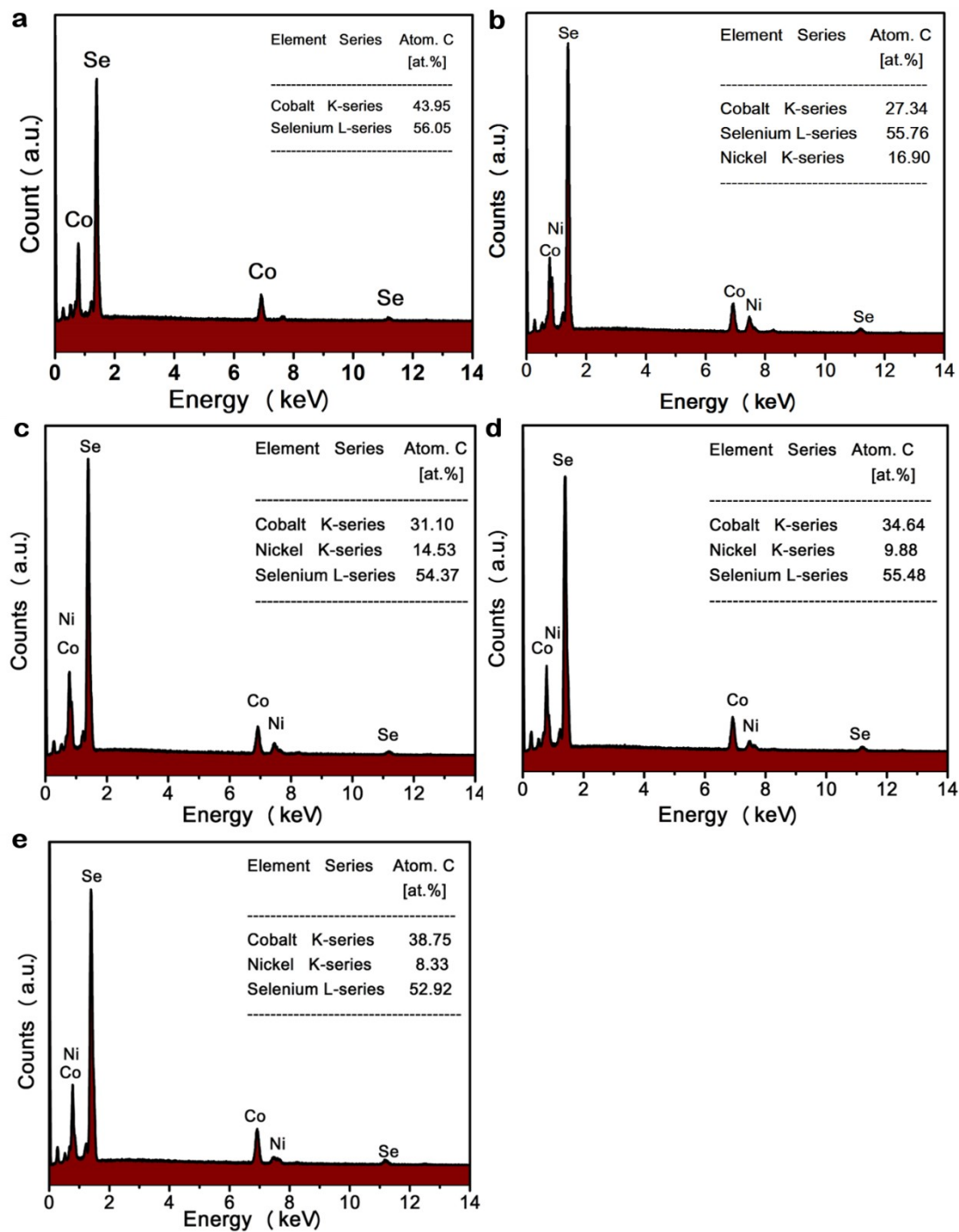


Fig. S3. EDX images of different samples. (a) Co_3Se_4 , (b) $\text{Ni}_{1.14}\text{Co}_{1.86}\text{Se}_4$, (c) $\text{Ni}_{0.95}\text{Co}_{2.05}\text{Se}_4$, (d) $\text{Ni}_{0.67}\text{Co}_{2.33}\text{Se}_4$, (e) $\text{Ni}_{0.53}\text{Co}_{2.47}\text{Se}_4$.

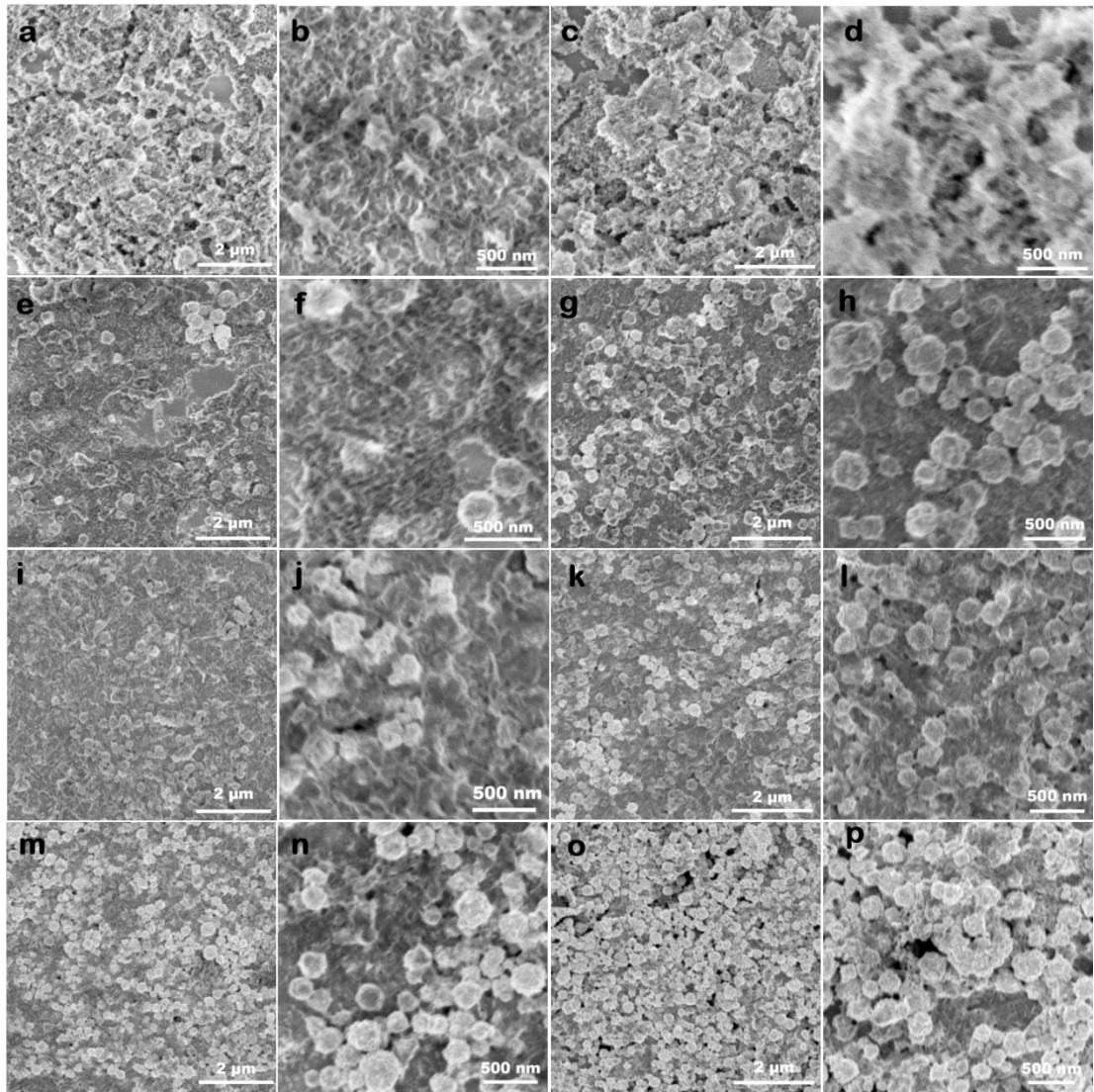


Fig. S4. SEM images of $\text{Ni}_{0.95}\text{Co}_{2.05}\text{Se}_4$ samples at different experimental conditions. (a-b) 100 °C, (c-d) 120 °C, (e-f) 140 °C, (g-h) 160 °C, (i-j) 1 h, (k-l) 3 h, (m-n) 6 h, (o-p) 9 h.

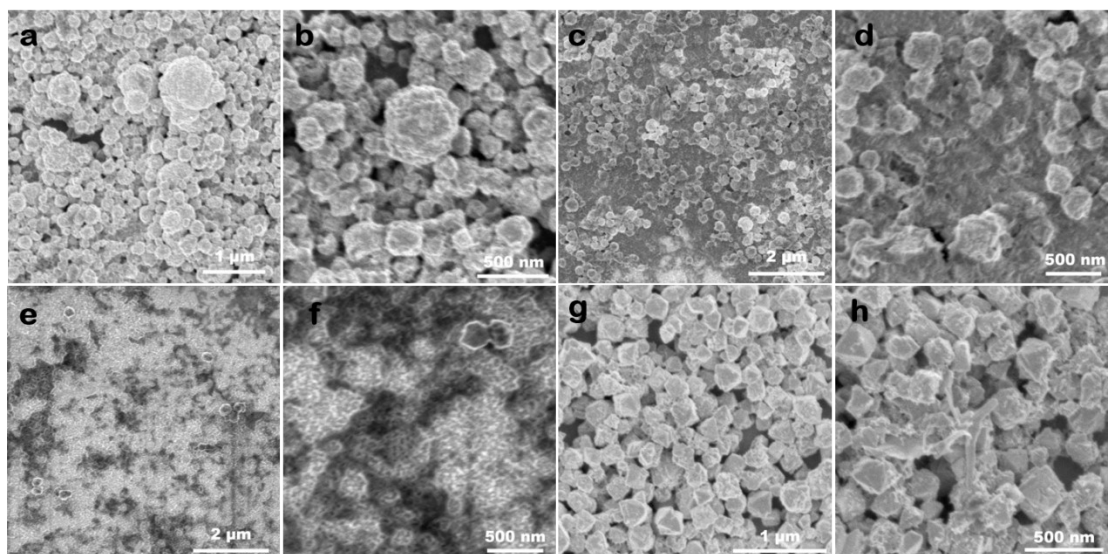


Fig. S5. SEM images of $\text{Ni}_{0.95}\text{Co}_{2.05}\text{Se}_4$ samples at different experimental conditions. (a-b) without cyclohexane, (c-d) without ethylene glycol, (e-f) without cyclohexane and ethylene glycol, (g-h) the ratio of nickel to cobalt is 2.2:1.

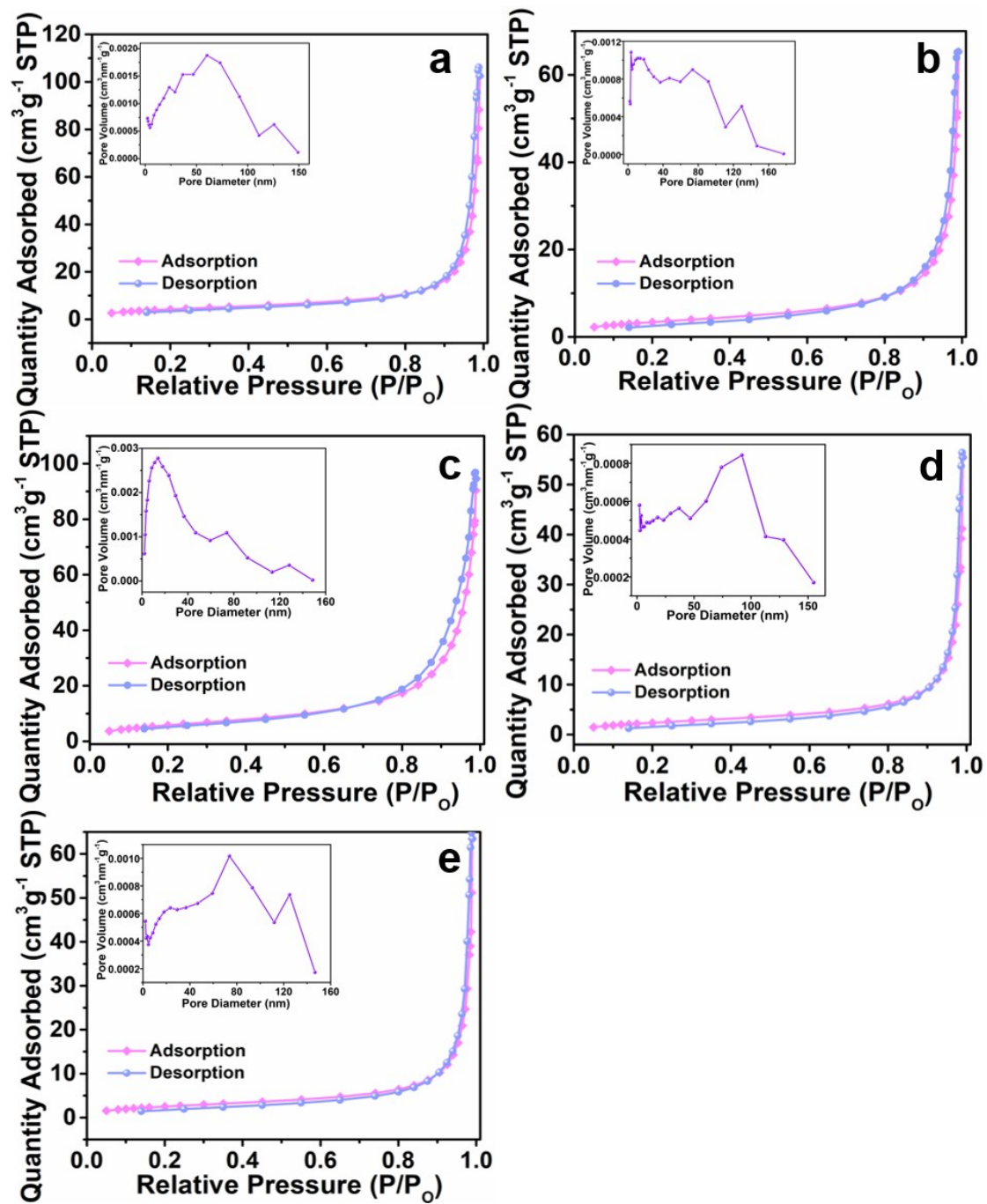


Fig. S6. N_2 sorption isotherms and the pore size distribution of different samples. (a) Co_3Se_4 , (b) $\text{Ni}_{1.14}\text{Co}_{1.86}\text{Se}_4$, (c) $\text{Ni}_{0.95}\text{Co}_{2.05}\text{Se}_4$, (d) $\text{Ni}_{0.67}\text{Co}_{2.33}\text{Se}_4$, (e) $\text{Ni}_{0.53}\text{Co}_{2.47}\text{Se}_4$.

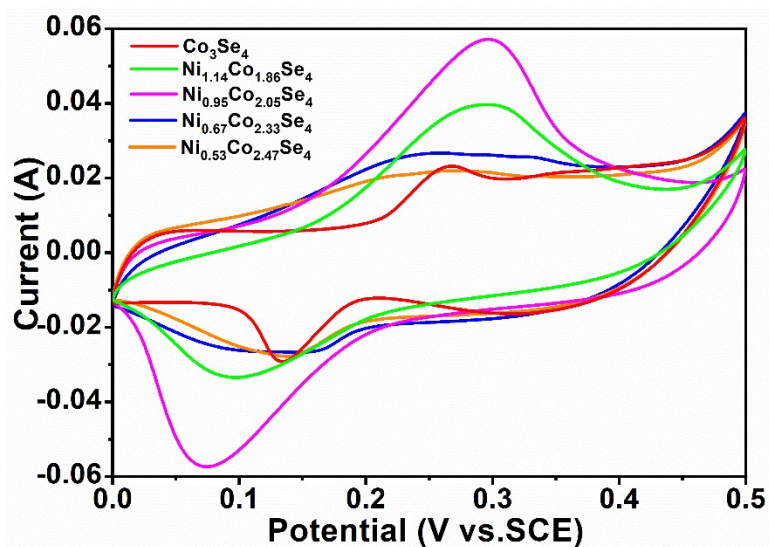


Fig. S7. CV curves of different proportions at the scanning speed of 20 mV s^{-1} .

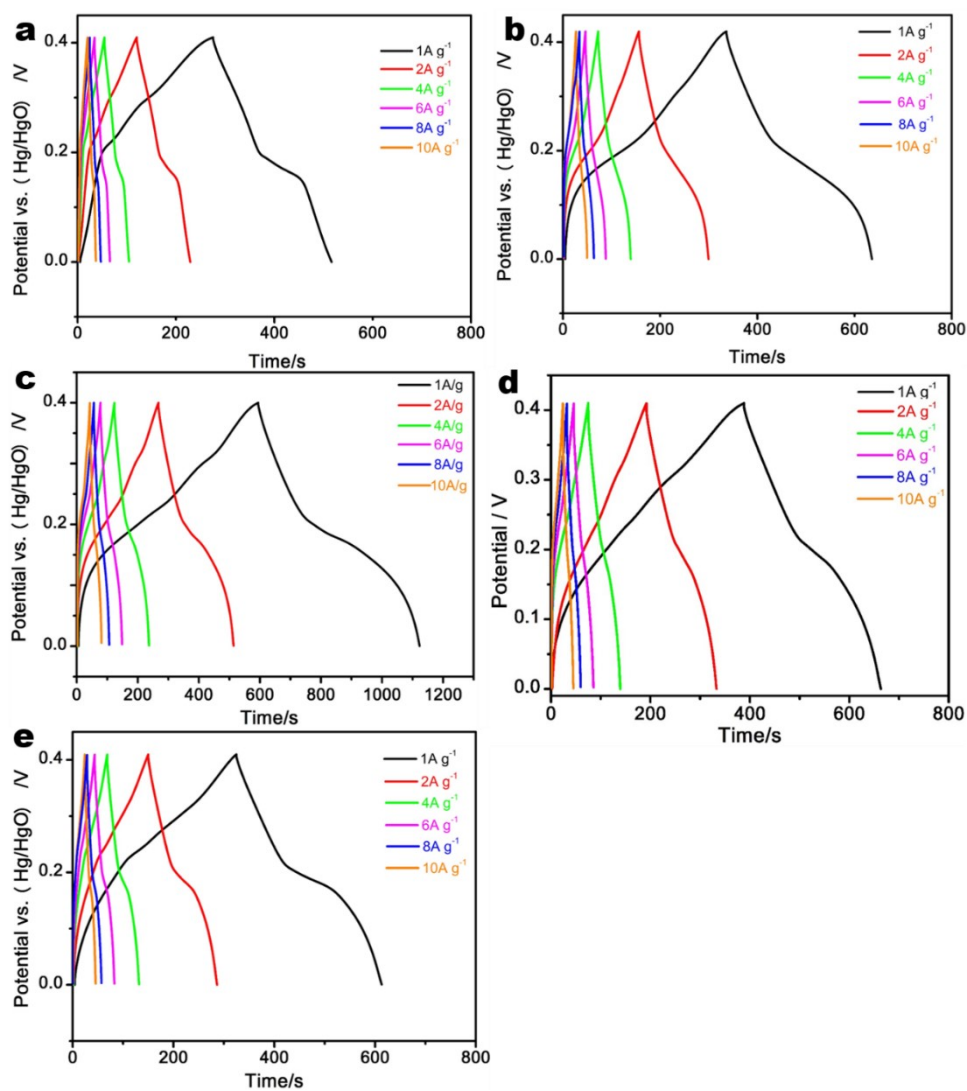


Fig. S8. GCD curves of different samples (a) Co_3Se_4 , (b) $\text{Ni}_{1.14}\text{Co}_{1.86}\text{Se}_4$, (c) $\text{Ni}_{0.95}\text{Co}_{2.05}\text{Se}_4$, (d) $\text{Ni}_{0.67}\text{Co}_{2.33}\text{Se}_4$, (e) $\text{Ni}_{0.53}\text{Co}_{2.47}\text{Se}_4$.

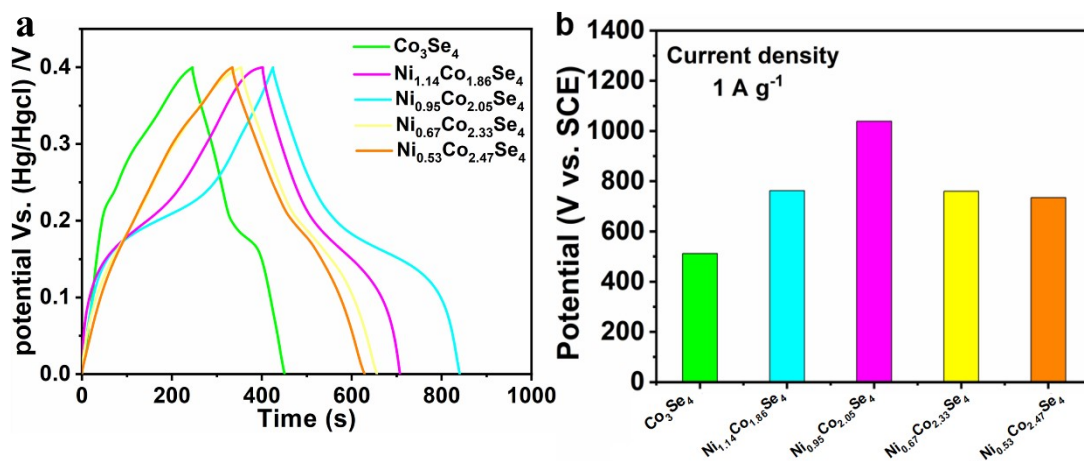


Fig. S9. GCD curves and capacity histogram of different samples at 1 A g⁻¹ current density.

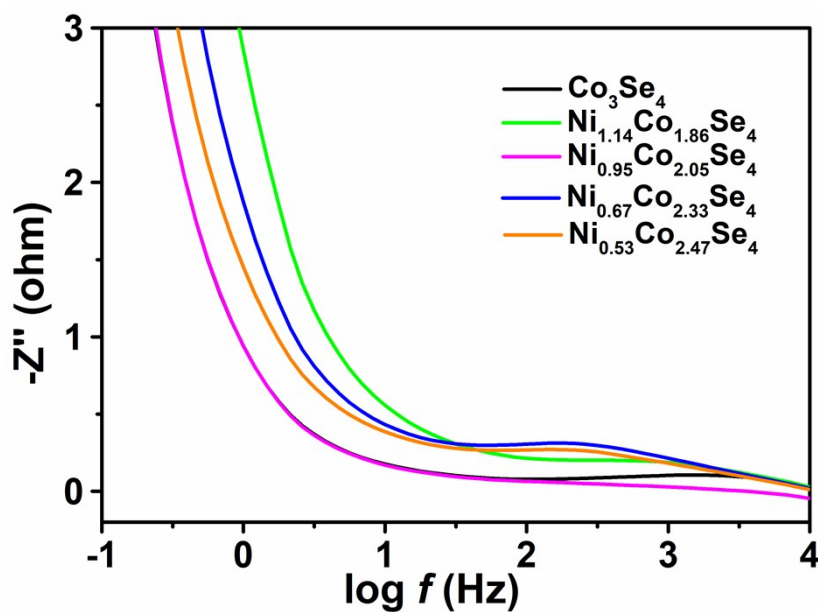


Fig. S10. Bode plot of (a) Co₃Se₄, (b) Ni_{1.14}Co_{1.86}Se₄, (c) Ni_{0.95}Co_{2.05}Se₄, (d) Ni_{0.67}Co_{2.33}Se₄, (e) Ni_{0.53}Co_{2.47}Se₄.

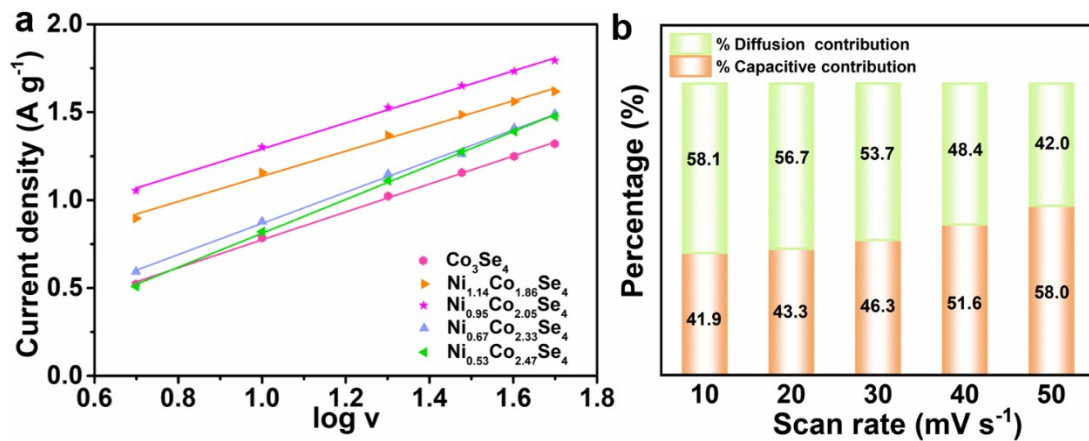


Fig. S11. (a) the fitting plots of log (current peak) versus log (scan rate) at oxidation peak of the series $\text{Ni}_x\text{Co}_{3-x}\text{Se}_4$ samples, (b) the diffusion and capacitive contribution of $\text{Ni}_{0.95}\text{Co}_{2.05}\text{Se}_4$ electrode at different scan rates.

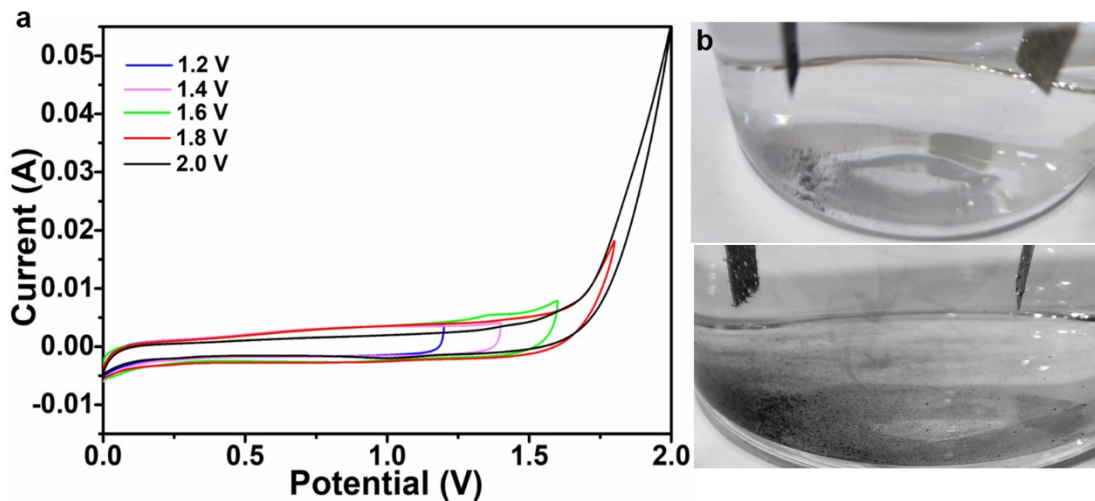


Fig. S12. (a) CV curves at different voltage windows of $\text{Ni}_{0.95}\text{Co}_{2.05}\text{Se}_4//\text{AC}$, (b) electrode conditions after CV testing at 1.8V and 2.0V.

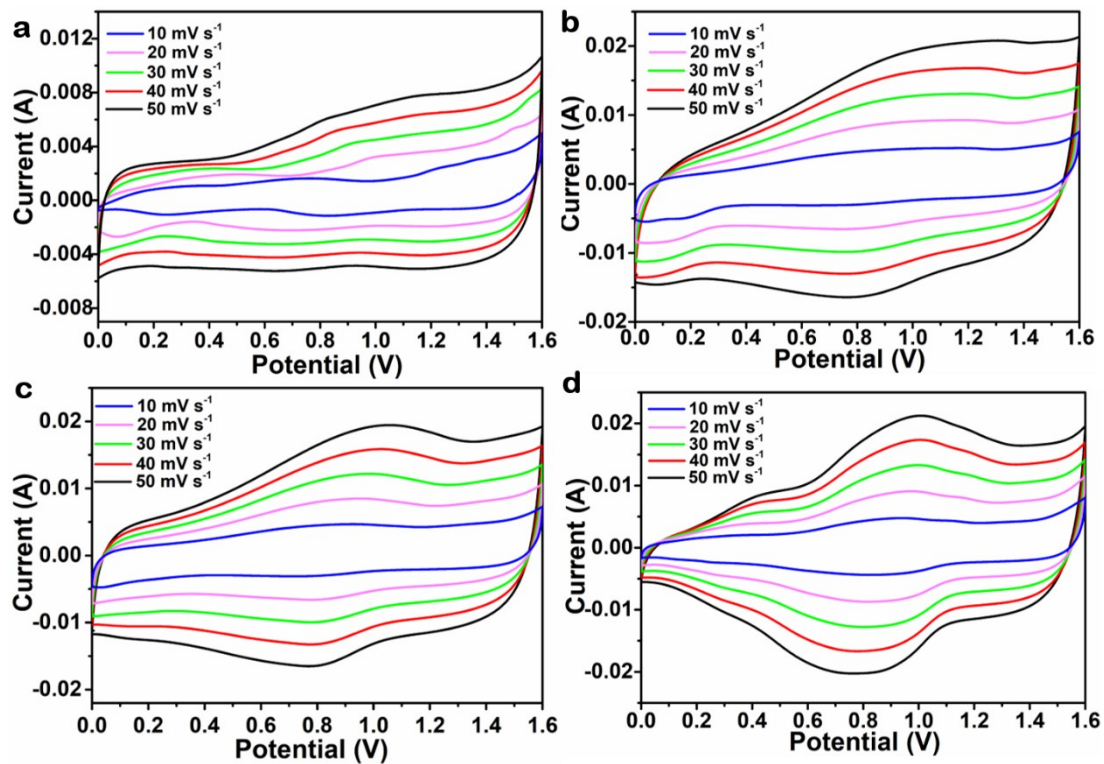


Fig. S13. CV curves of different samples (a) Co_3Se_4 , (b) $\text{Ni}_{1.14}\text{Co}_{1.86}\text{Se}_4$, (c) $\text{Ni}_{0.67}\text{Co}_{2.33}\text{Se}_4$, (d) $\text{Ni}_{0.53}\text{Co}_{2.47}\text{Se}_4$.

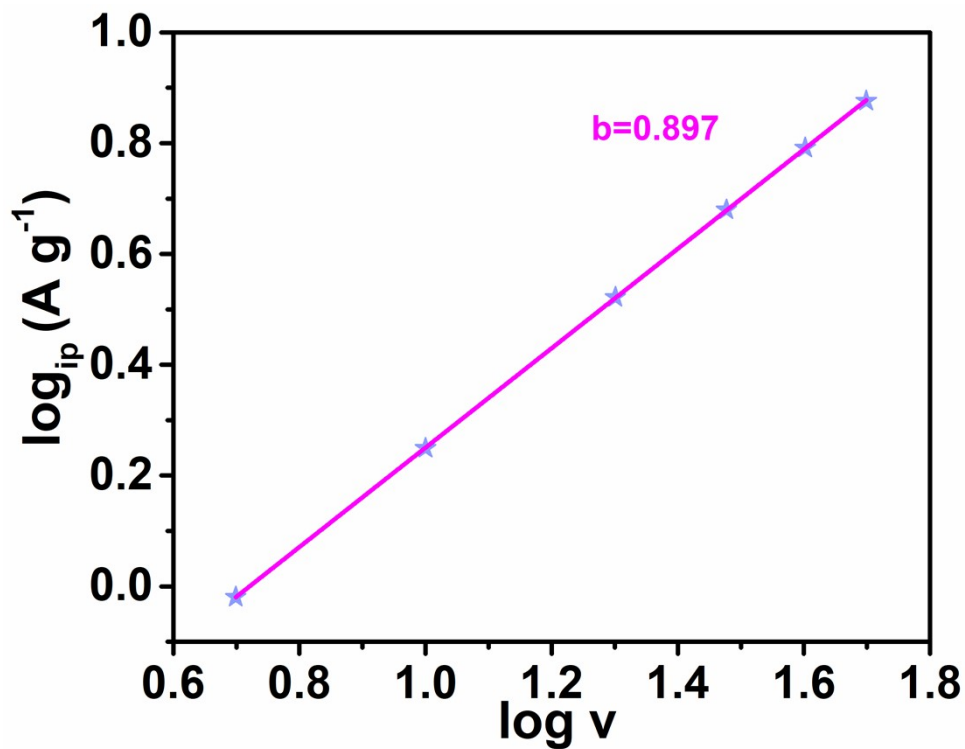


Fig. S14. Log (i) vs log (v) plots of $\text{Ni}_{0.95}\text{Co}_{2.05}\text{Se}_4//\text{AC}$ electrode.

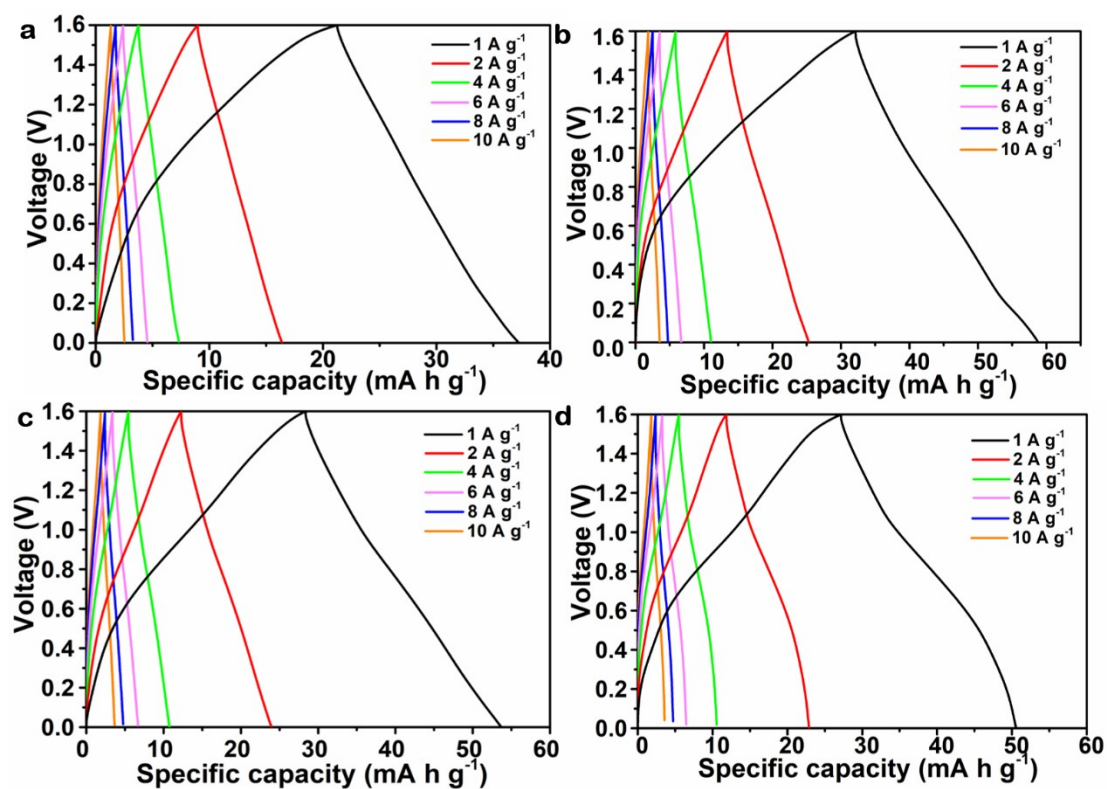


Fig. S15. GCD curves of different samples (a) $\text{Co}_3\text{Se}_4//\text{AC}$, (b) $\text{Ni}_{1.14}\text{Co}_{1.86}\text{Se}_4//\text{AC}$, (c) $\text{Ni}_{0.67}\text{Co}_{2.33}\text{Se}_4//\text{AC}$, (d) $\text{Ni}_{0.53}\text{Co}_{2.47}\text{Se}_4//\text{AC}$.

Table S1. Different sample sizes and average sizes.

Sample names	Max/Min sizes (nm)	Average sizes
Co_3Se_4	261.36/143.86	190.56
$\text{Ni}_{1.14}\text{Co}_{1.86}\text{Se}_4$	288.98/145.40	213.10
$\text{Ni}_{0.95}\text{Co}_{2.05}\text{Se}_4$	256.94/124.78	193.85
$\text{Ni}_{0.67}\text{Co}_{2.33}\text{Se}_4$	400.26/167.59	242.89
$\text{Ni}_{0.53}\text{Co}_{2.47}\text{Se}_4$	299.10/141.81	222.28

Table S2. The fitting values resistance of these samples.

Sample names	R_s (Ω)	R_{ct} (Ω)	$D(\text{cm}^2 \text{s}^{-1})$
Co_3Se_4	1.142	0.677	3.694×10^{-9}
$\text{Ni}_{1.14}\text{Co}_{1.86}\text{Se}_4$	0.717	1.735	1.098×10^{-9}
$\text{Ni}_{0.95}\text{Co}_{2.05}\text{Se}_4$	1.011	0.242	4.843×10^{-9}
$\text{Ni}_{0.67}\text{Co}_{2.33}\text{Se}_4$	0.947	0.433	3.673×10^{-9}
$\text{Ni}_{0.53}\text{Co}_{2.47}\text{Se}_4$	0.927	0.339	9.260×10^{-10}

Table S3. The comparison of electrochemical performances between Ni-Co selenide electrodes with the reported selenide related electrodes.

Materials	Specific capacity, F g ⁻¹ /Cycle numbers, (Current density, A g ⁻¹)	Voltage (V)	Electrolyte concentration (KOH, mol)	Reference
H-NiCoSe ₂ sub-microspheres	608 /5000 th , (10)	0.5	6	S1
GeSe ₂	297.9 /2000 th , (1)	0.1-0.65	1	S2
Ni-Co-Se-2	382.33 /2000 th , (5)	0.6	6	S3
NiCo _{2.1} Se _{3.3} NSs/3D G/NF	395.36 /1000 th , (10A cm ⁻²)	0.6	6	S4
Ni _{0.5} Co _{0.5} Se ₂	1007/3500 th , (7)	0.55	6	S5
Co ₃ Se ₄	426.75/4000 th , (4)	0.5	2	
Ni _{1.14} Co _{1.86} Se ₄	493.47/4000 th , (4)	0.5	2	
Ni _{0.95} Co _{2.05} Se ₄	625.27/4000 th , (4)	0.5	2	This work
Ni _{0.67} Co _{2.33} Se ₄	468.2/4000 th , (4)	0.5	2	
Ni _{0.53} Co _{2.47} Se ₄	561.44/4000 th , (4)	0.5	2	

Supplementary References

1. L. R. Hou, Y. Y. Shi, C. Wu, Y. R. Zhang, Y. Z. Ma, X. Sun, J. F. Sun, X. G. Zhang and C. Z. Yuan, Monodisperse Metallic NiCoSe₂ Hollow Sub-Microspheres: Formation Process, Intrinsic Charge-Storage Mechanism, and Appealing Pseudocapacitance as Highly Conductive Electrode for Electrochemical Supercapacitors, *Adv. Funct. Mater.*, 2018, 28, 1705921.
2. X. F. Wang, B. Liu, Q. F. Wang, W. F. Song, X. J. Hou, D. Chen, Y. B. Cheng, G. Z. Shen, Three-dimensional hierarchical GeSe₂ nanostructures for high performance flexible all-solid-state supercapacitors, *Adv. Mater.*, 2013, 25, 1479-1486.

3. S. Li, Y. J. Ruan, Q. Xie, Morphological modulation of NiCo₂Se₄ nanotubes through hydrothermal selenization for asymmetric supercapacitor, *Electrochim. Acta*, 2020, 356, 136837.
4. Y. X. Wang, W. J. Zhang, X. L. Guo, K. Jin, Z. T. Chen, Y. Y. Liu, L. L. Yin, L. Li, K.B. Yin, L. T. Sun, Y. H. Zhao, Ni-Co selenide nanosheet/3D graphene/nickel foam binder-free electrode for high-performance supercapacitor, *ACS Appl Mater. Interfaces*, 2019, 11, 7946-7953.
5. X. X. Song, C. H. Huang, Y. L. Qin, H. L. Li, H. C. Chen, Hierarchical hollow, sea-urchin-like and porous Ni_{0.5}Co_{0.5}Se₂ as advanced battery material for hybrid supercapacitors, *J. Mater. Chem. A*, 2018, 6, 16205-16212.